Research Article

Pulmonary Circulation

Sugen–morphine model of pulmonary arterial hypertension

Stuti Agarwal[1,*], Zachery J. Harter[1,*], Balaji Krishnamachary[1], Ling Chen[1], Tyler Nguyen[1], Norbert F. Voelkel[2] and Navneet K. Dhillon[1]

[1]Department of Internal Medicine, University of Kansas Medical Center, Kansas City, KS, USA; [2]Department of Pulmonary Sciences, Vrije University Medical Center, Amsterdam, The Netherlands

Abstract

Pulmonary arterial hypertension is a fatal disease associated with pulmonary vascular remodeling and right ventricular hypertrophy. Pre-clinical animal models that reproduce the human pulmonary arterial hypertension process and pharmacological response to available therapies are critical for future drug development. The most prevalent animal model reproducing many aspects of angioobliterative forms of pulmonary arterial hypertension is the rat Sugen/hypoxia model in which Sugen, a vascular endothelial growth factor receptor antagonist, primarily causes initiation of endothelial injury and later in the presence of hypoxia promotes proliferation of apoptosis-resistant endothelial cells. We previously demonstrated that exposure of human pulmonary microvascular endothelium to morphine and HIV-proteins results in initial apoptosis followed by increased proliferation. Here, we demonstrate that the double-hit of morphine and Sugen 5416 (Sugen–morphine) in rats leads to the development of pulmonary arterial hypertension with significant medial hypertrophy of pre-acinar pulmonary arteries along with neo-intimal thickening of intra-acinar vessels. In addition, the pulmonary smooth muscle and endothelial cells isolated from Sugen–morphine rats showed hyperproliferation and apoptotic resistance, respectively, in response to serum starvation. Our findings support that the dual hit model of Sugen 5416 and morphine provides another experimental strategy to induce significant pulmonary vascular remodeling and development of severe pulmonary arterial hypertension pathology in rats without exposure to hypoxia.

Keywords

endothelial cells, pulmonary vascular remodeling, vascular endothelial growth factor receptor (VEGFR), proliferation, pulmonary hypertension

Date received: 3 May 2019; accepted: 11 December 2019

Pulmonary Circulation 2020; 10(1) 1–9
DOI: 10.1177/2045894019898376

Introduction

Pulmonary arterial hypertension (PAH), Group 1 of the pulmonary hypertension (PH) classification, comprises multiple etiologies such as drug-induced PAH[1] and HIV-related PAH,[2] as well as hereditary (e.g. Bone Morphogenetic Protein Receptor II) and idiopathic forms.[3] Regardless of the etiology, PAH is a progressive and incurable disease of the pulmonary vasculature characterized by sustained pulmonary vasoconstriction and pulmonary vasculature remodeling of pre-capillary arterial vessels that eventually progresses to right ventricular remodeling, right heart failure, and death.[4] Preclinical animal models have, over the last decades, contributed substantially to unraveling the complex pathophysiology and pathobiology of PH.[5] In spite of these accomplishments, no available therapeutic options consistently improve the (mal)adapted right ventricular function or reverse the established plexogenic arteriopathy.[6] Current knowledge using high pressure (increased right ventricle (RV) afterload) PAH animal models still lack an understanding of the RV-pulmonary axis and progression of RV dysfunction, as well as the pathophysiological

*These authors contributed equally to this work.

Corresponding author:
Navneet K. Dhillon, Division of Pulmonary and Critical Care Medicine, Department of Medicine, Mail Stop 3007, University of Kansas Medical Center, 3901 Rainbow Blvd, Kansas City, KS 66160, USA.
Email: ndhillon@kumc.edu

role that angio-obliterative pulmonary vasculature remodeling plays in RV failure.[7]

Of the PH animal models reviewed recently,[6] the most commonly utilized plexogenic arteriopathy PAH rat model that most closely mimics the human phenotype is the Sugen 5416 (SU5416)/hypoxia/normoxia model.[8] SU5416 is a potent and selective vascular endothelial growth factor (VEGF) receptor 1[9] and 2[10] antagonist. It has been well established that SU5416 primarily causes initial endothelial cell (EC) injury and later hyperproliferation of apoptosis-resistant ECs,[11] a characteristic of angio-obliterative (plexiform/complex) lesion formation in the development of severe PAH.[11] However, a recent study suggests that pulmonary EC injury alone is insufficient to cause severe PAH, thus highlighting the requirement of additional factors in the development of PAH[12] and importance of a "double-hit or multiple hits" mechanism that also applies to PAH animal models.[2,13–16]

Similar to the injurious effects of SU5416 on pulmonary ECs, morphine has been shown to cause both apoptosis and proliferation of vascular ECs.[17–19] We previously reported that the combination of morphine with HIV-infection accentuates pulmonary vascular remodeling characterized by formation of neointimal fibrotic or plexiform lesions in Simian Immunodeficiency Virus (SIV)-infected *Rhesus macaques*.[20] In addition, our laboratory has reported that morphine and HIV-proteins cause initial endothelial apoptosis which is followed by proliferation of primary human pulmonary microvascular ECs; these events corresponded to an initial inactivation of VEGF receptor (VEGFR) and a later increase in VEGFR phosphorylation during chronic exposure to morphine and HIV-protein.[20,21]

Here, we hypothesize that a double-hit of SU5416 and morphine may induce PAH in wild-type rats and potentially serve as a new PAH animal model. This study aims to develop a preclinical animal model of PAH that recapitulates altered hemodynamic and remodeled vasculature phenotypes that characterize PAH in human patients.

Material and methods

Animals

Male Sprague Dawley (SD) rats ($n = 10$–12/group) weighing 180–220 g (ENVIGO, Indianapolis, IN, USA) were administered a single subcutaneous (SC) injection of SU5416, 20 mg/kg body weight (SU5416, Cayman Chemicals, USA) with intraperitoneal (IP) injections of morphine (10 mg/kg body weight; Sigma) once daily for 35 days (Sugen–morphine (SuMo) group) or were administered only SU5416 once (Sugen group) or only morphine (morphine group) for 35 days. The control rats were administered vehicle for SU5416 (1% carboxymethylcellulose in saline with 0.4% Tween-80) once (SC) followed by IP injections of saline, once daily for 35 days. The animals were housed at the University of Kansas Medical Center (Kansas City, KS) in strict accordance with the National Institutes of Health (NIH) and Institutional Animal Care and Use Committee guidelines. Water and food were available ad libitum and the animals were housed individually under 12 h/12 h light–dark cycle.

Catheterization and hemodynamics

Animals were anesthetized with a Ketamine/Xylazine mixture (50 mg/kg:10 mg/kg, IP) and a midline incision was then made near the neck region (ventral position) to insert the catheters into the left carotid artery and right jugular vein. A polyethylene catheter (BD Intramedic™, Clay Adams®, PE 50 (Inner Diameter: 0.58 mm, Outer Diameter: 0.965 mm)—ADInstruments) was placed in the aortic arch via the left carotid artery, and a Millar 2.0 F single pressure catheter (ADInstruments, Millar Instruments, SPR-513 Mikro-Tip®, Houston, TX) was advanced into the RV through the right jugular vein. The adequate placement of the catheters was established by the pressure waveform. Mean arterial pressure (MAP) and RV systolic pressure (RVSP) were measured on PowerLab Data Acquisition System (ADInstruments Inc., Colorado Springs, CO, USA) and analyzed with the LabChart System (AD Instruments Inc., Version 8.0 Pro, Colorado Springs, CO, USA).

Tissue harvesting

After hemodynamic measurements, the rats were euthanized by exsanguination through the carotid artery. The catheter was then removed, and the incision was extended to open the thorax. Lungs were perfused first with normal saline followed by whole body perfusion. The lung block was removed, and the RV free wall of the heart was separated from the left ventricle (LV) and weighed separately on a digital scale. The RV/LV + septum ratio (Fulton Index) was then calculated to assess the RV hypertrophy (RVH).[22] A part of the RV and LV + septum was fixed in 4% paraformaldehyde for histological and immunohistochemistry analysis. The remaining heart tissue was snap frozen in liquid nitrogen. Similarly, the lung lobes were dissected, and the left lobe was snap frozen in liquid nitrogen for EC isolation, RNA, and protein analysis, while the right lobe was fixed in 4% paraformaldehyde for histological evaluation as described elsewhere.[23]

Histochemical analysis

Paraformaldehyde-fixed lungs were paraffin-embedded and sectioned. Prior to staining, the deparaffinization of sections was carried out in xylene, followed by rehydration in ethanol and then antigen retrieval in citrate buffer. Immunohistochemical staining was performed for smooth muscle cells (SMCs) with α-smooth muscle actin (Abcam, USA), ECs with von Willebrand Factor VIII (vWF)

marker (DakoCytomation, USA), and cell proliferation marker—proliferating cell nuclear antigen (PCNA) (Cell Signaling Technology, USA). Immunofluorescence staining of the lung tissue sections was performed to check the VEGFR3 (Novus Biologicals, USA) expression. For immunofluorescence, AlexaFluor 488 and 594 (ThermoScientific Corporation, USA) were used for anti-rabbit and anti-mouse secondary antibody, respectively, and 4', 6-diamidino-2-phenylindole was used to stain the nuclei. Trichrome staining was carried out on the RV paraffin-embedded fixed sections to assess the collagen deposition in the RV.

Morphometric analysis

Quantification of vessel thickness was done by scanning the paraffin-embedded slides into the Aperio® System. Subsequently, pulmonary vessels were divided into three groups based on diameter: those greater than 100 μm, between 50 and 100 μm, and less than 50 μm. Wall thickness was determined by measuring the difference between the outer diameter and inner diameter of each vessel and was compared by equation: Median Wall Thickness = External Area – Internal Area. Approximately 12–15 vessels per lobe from each size group were measured per rat and then averaged.

Cardiomyocyte thickness was measured by calculating the width of the cardiomyocytes of animals from each group. Around 10 fields were imaged per section, and the cardiomyocytes that were present in a similar orientation with no change in width were measured for thickness from the center of the nucleus. Approximately 30–40 cardiomyocytes were measured and averaged for each animal per group to get the average cardiomyocyte size.

Isolation of rat pulmonary arterial SMCs and microvascular ECs

Rat pulmonary arterial SMCs (RPASMCs) were cultured from isolated pulmonary artery. Briefly, the pulmonary artery was digested with collagenase and elastase, and cultured on six-well plates in rat smooth muscle cell media (SMCM) (Cell Applications, USA).

Rat pulmonary microvascular ECs (RPMECs) were isolated from lung lobe. Briefly, the lung tissue was washed in chilled Dulbecco's Minimum Essential Medium, chopped, and digested with collagenase. The suspension was then passed through 18G syringe to make single cell suspension and nylon cell strainer (BD Biosciences, USA). The cells were then treated with EC-specific antibodies CD31, CD105, and biotin-conjugated Isolectin B4 and subsequently with IgG and streptavidin Magnetic-activated cell sorting (MACS) microbeads (Miltenyi Biotec, USA). The magnetic bead-labeled ECs were then pulled using MACS Cell Separation columns (Miltenyi Biotec, USA). The cells were cultured on six-well plate in rat endothelial cell media (ECM) (Cell Applications, USA) and used for further experiments.

Cell proliferation and apoptosis assays

For analysis of proliferation in isolated rat cells, both RPASMCs and RPMECs (3×10^3 cells/well) from control, Sugen, morphine, and SuMo groups of rats were plated on 96-well plates and grown in complete rat SMCM and ECM, respectively. For RPASMCs, complete SMCM was replaced after 48 h with 0.1% Fetal Bovine Serum (FBS) containing SMCM for 48 h to make them quiescent. Fresh 0.1% FBS containing SMCM was added to the cells, and CellTiter 96® Aqueous One Solution Cell Proliferation Assay (Promega, Madison, WI) and CyQuant Assay were performed at day 2. For RPMECs, after 24 h, the media was changed to 0.5% containing ECM. Cell proliferation assay was performed at days 2 and 4 according to the manufacturer's instructions. For analysis of apoptosis, 1.25×10^4, RPMECs/well were plated on 96-well plates in complete rat ECM. After 24 h, the media was changed to 0.5% serum containing media. Cell death/oligonucleosome detection ELISA (Millipore Sigma, USA) was performed after 24 and 48 h according to the manufacturer's instructions.

Western blot analysis

Total protein was isolated from flash-frozen rat lung tissues using radio immunoprecipitation assay lysis buffer followed by Western Blot for VEGFR2 (Cell Signaling Technology, USA) and VEGFR3 (Abcam, USA) expression. The NIH ImageJ software was used for densitometry analysis of immunoblots.

Statistical analysis

Statistical analysis was performed using one-way analysis of variance with post-hoc Bonferroni correction for multiple comparisons. p Values were calculated for all the analysis using GraphPad Prism 7 software. Results were judged statistically significant when the Bonferroni corrected p value was less than 0.05. For correlation analysis, one-tailed Pearson correlation coefficient was calculated using GraphPad Prism 7 software, and significance was assessed as $p < 0.05$.

Results

The combination of morphine with Sugen exacerbates the increase in right ventricular pressure of morphine-treated rats

We compared the hemodynamic measurements in SD rats treated with SuMo (SuMo group), Sugen only (Sugen group), or morphine only (morphine group) with untreated control rats. As shown in Fig. 1(a), there was a significant

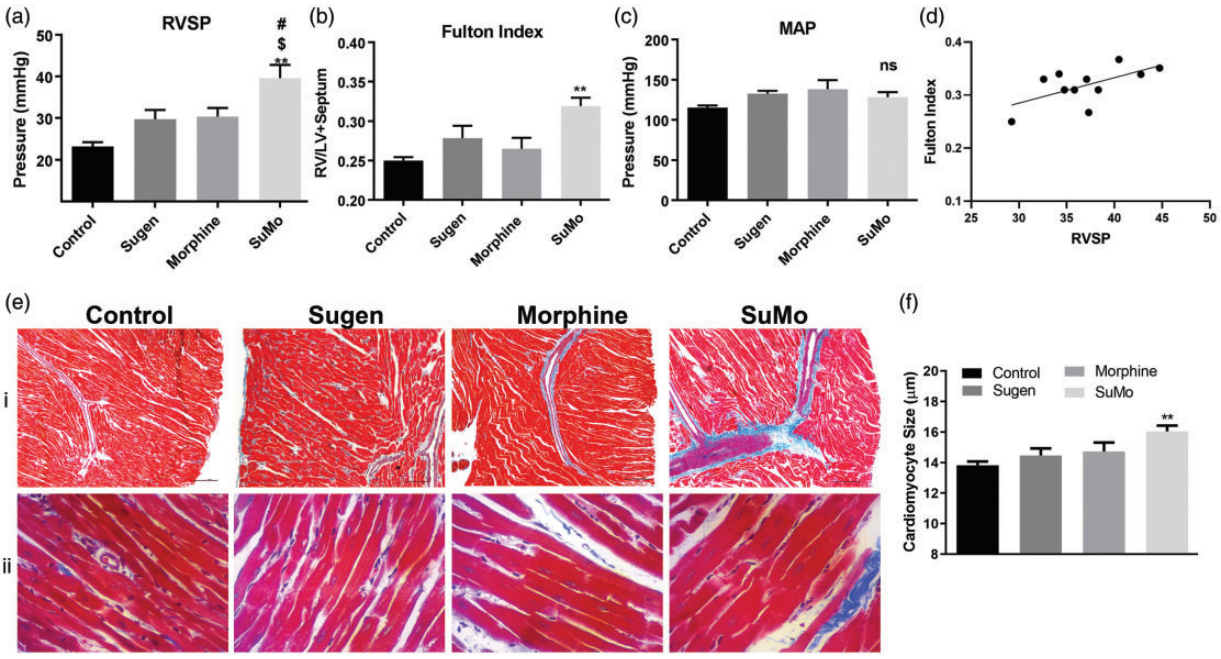

Fig. 1. Hemodynamics and RV hypertrophy in SD rats exposed to Sugen and morphine. Sprague Dawley rats were administered 20 mg/kg Sugen5416 once and/or 10 mg/kg body weight of morphine daily for 35 days. Untreated controls were used for comparison. (a) Right ventricle systolic pressure (RVSP); (b) Fulton Index; and (c) mean arterial pressure from $n = 7$ or more rats per group. Values are mean ± SEM. (d) Correlation between RVSP and Fulton Index (Pearson correlation coefficient $r = 0.6165$, $p = 0.0217$, $n = 11$ rats). (e) Masson's trichrome staining on formaldehyde-fixed, paraffin-embedded heart RV sections: (i) magnification 4 × and (ii) magnification 40×; (f) Quantification of cardiomyocyte size in Sugen and/or morphine-exposed rats.
Notes: Values are mean ± SEM obtained from $n = 6$ rats per group.
**: $p < 0.01$, vs control; #: $p < 0.05$ vs Sugen; $: $p < 0.05$ vs morphine; MAP: mean arterial pressure; SuMo: Sugen–morphine.

increase in the RVSP measurement in SuMo group when compared to the control group as well as the Sugen or morphine alone groups. In contrast, there was no change in MAP among all the four groups suggesting that the systemic blood pressure did not contribute to the RV changes (Fig. 1(c)). A significant RVH was also observed in the SuMo group when compared to the control group as demonstrated by a significant increase in the Fulton Index (RV/LV + Septum ratio) (Fig. 1(b)) that showed significant correlation with increasing RVSP (Fig. 1(d)). The trichrome staining of the RV demonstrated increased collagen deposition and fibrosis in the SuMo group when compared to the control or SuMo only groups (Fig. 1(e i)). Furthermore, a significant increase in the cardiomyocyte size was associated with an increase in the RVH in the SuMo group when compared to the control group (Fig. 1(e ii) and (f)).

Enhanced pulmonary vascular remodeling in SuMo rats

As presented in Fig. 2 (a)–(c), increased thickening of the smooth muscle layer was observed in both pre-acinar and intra-acinar pulmonary arteries from the SuMo group as compared with the other three groups. The median wall thickness of the SMC layer of vessels < 50 μm, 50–100 μm and >100 μm was calculated for all the four groups. Of all the three groups of vessels, only the median wall thickness of vessels >100 μm was observed to be significantly higher in rats from SuMo group as compared to the controls (Fig. 2(d)). Nevertheless, 50–100 μm and <50 μm size vessels also showed the trend of increased thickness in the SuMo group. Additionally, greater extent of vessel muscularization was observed in the rats from SuMo group with a significant increase in the number of completely or partially muscularized vessels of size < 50 μm (Fig. 2(e)) when compared with other groups. We also observed many partially occluded vessels due to increased smooth muscle proliferation and in some cases due to increase in endothelial proliferation and blebbing of ECs in the SuMo group (Fig. 2(b)). Staining for the expression of PCNA provided evidence for the presence of proliferative ECs within the intra-acinar arterioles (Fig. 2(c)). These results suggest that morphine acts as a second hit when combined with SU5416 in stimulating EC proliferation as well as smooth muscle thickening in the pulmonary vessels leading to development of PAH.

Increased survival and proliferation of pulmonary smooth muscle and ECs isolated from SuMo rats

We next tested the survival and proliferative ability of isolated RPASMCs and RPMECs upon serum starvation. The RPASMCs from SuMo rats showed a significantly higher

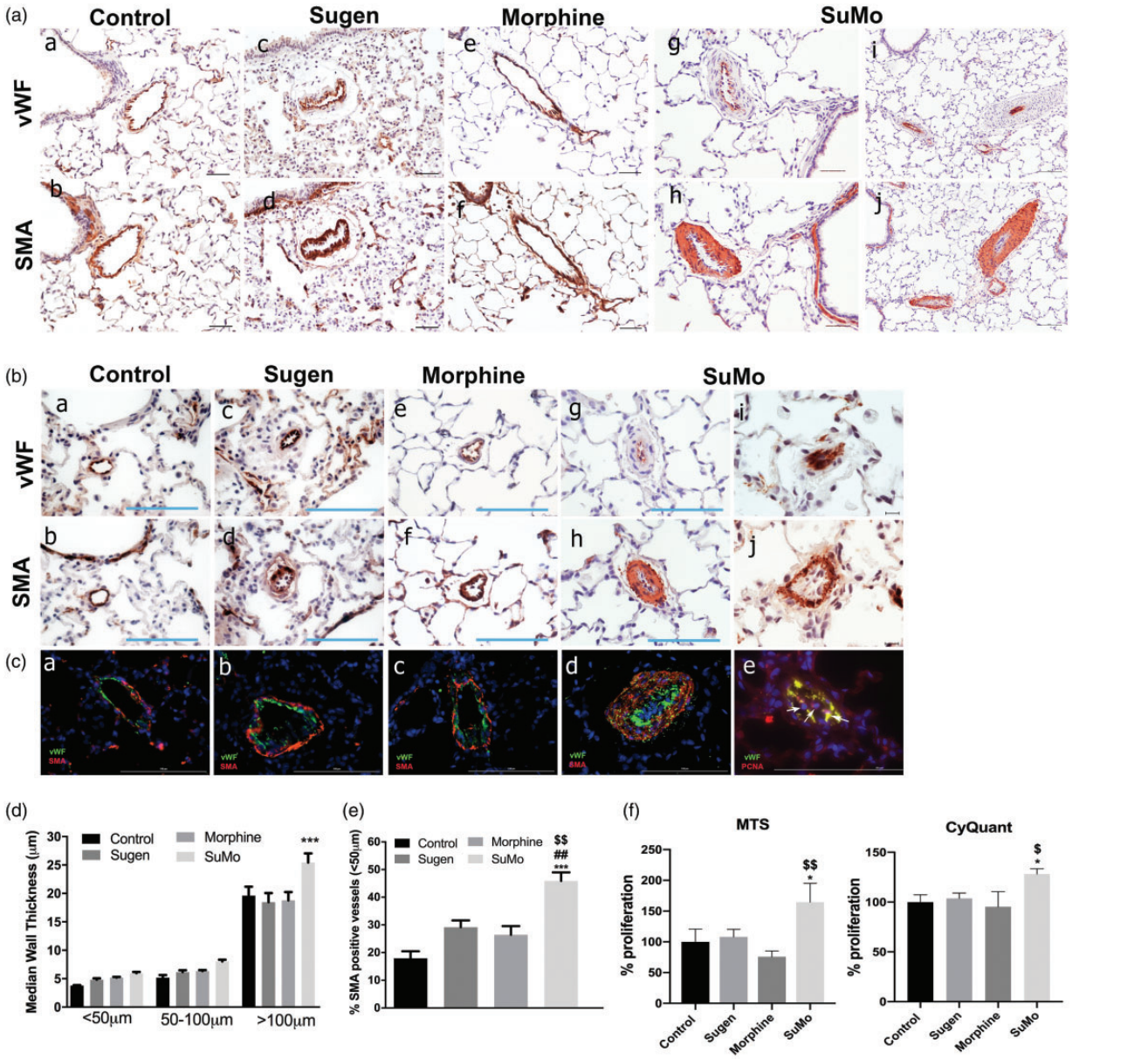

Fig. 2. Immunohistochemical analysis of pulmonary vessels in SD rats exposed to Sugen and morphine. Right lung was harvested, fixed, paraffin-embedded, and sectioned followed by immune-staining for von Willebrand factor (vWF) and α-smooth muscle actin (α-SMA). (a) and (b): Representative pictographs showing remodeled pulmonary vessels of size 50–100 μm; (a)–(h): magnification 20×, Scale bar = 100 μm; (i)–(j): magnification 10×, Scale bar = 100 μm); and (b) intra-acinar vessels of size < 50 μm (a)–(h): magnification 40×, Scale bar = 100 μm; (i)–(j): magnification 60×, Scale bar = 100 μm). (C) Immunofluorescence staining of vWF (green)/α-SMA (red) ((a)–(d)); and vWF (green)/PCNA (red) in intra-acinar pulmonary vessels (e) Scale bar = 100 μm. (D) Median smooth muscle wall thickness was assessed by measuring inner and outer diameter of remodeled arteries and arterioles. Values are mean ± SEM of $n = 6$ rats per group. (E) Extent of muscularization in vessels < 50 μm size was assessed by counting α-SMA positive vessels and total number of vessels in the right lung lobe from all groups and plotted as percent muscularized vessels. Values are mean ± SEM of $n = 4$ rats per group. (F) RPASMCs were plated on 96-well plates using complete SMCM and were made quiescent for 48 h by changing to 0.1% serum containing media. MTS and CyQuant proliferation assay was performed at day 2 post starvation.

Notes: Values are mean ± SEM obtained from $n = 3$ rats.

***: $p < 0.001$, *: p<0.05 vs control; ##: p<0.01 vs Sugen; $$: p<0.01, $: p<0.05 vs Morphine SuMo: Sugen–morphine.

proliferation when compared with control and morphine-treated rats as confirmed by both MTS and CyQuant assay (Fig. 2(f)). In addition, RPMECs from SuMo rats showed cell death resistance and better survival upon serum starvation when compared to the control group, both at 24 h and 48 h of serum starvation as determined by cell death ELISA (Fig. 3(a)). Furthermore, RPMECs from SuMo rats also demonstrated enhanced proliferation

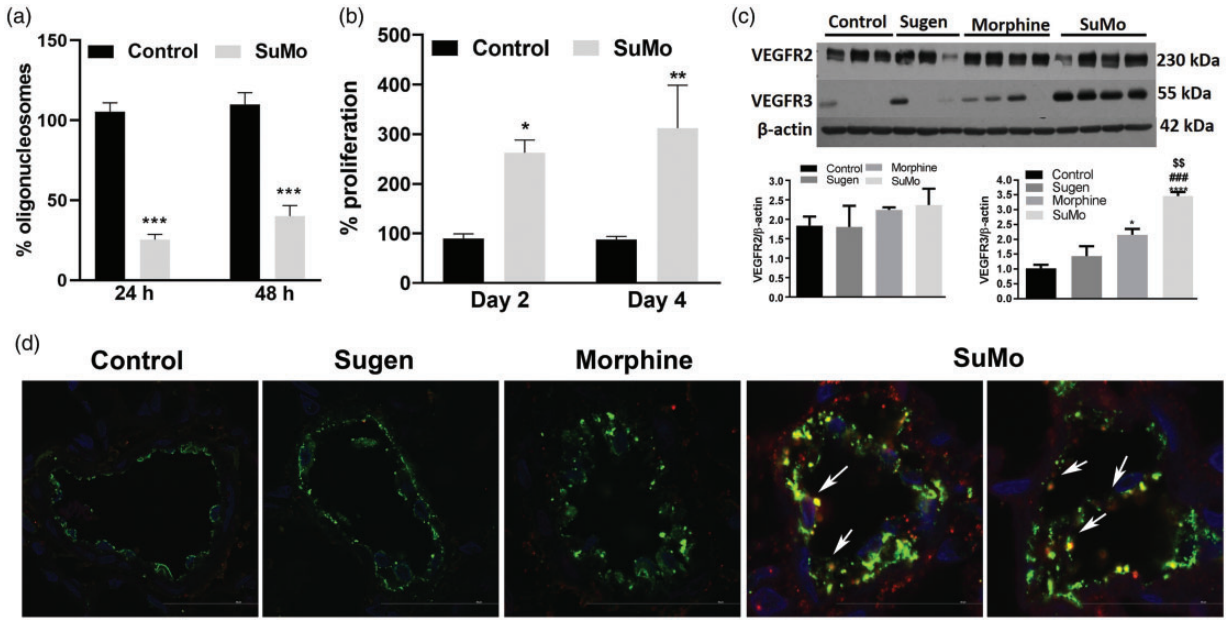

Fig. 3. Proliferation in RPMECs and VEGFR expression in SD rats exposed to Sugen and morphine. RPMECs were plated on 96-well plates using complete ECM and were starved next day by changing to 0.5% serum containing media. (a) Cell death detection ELISA was performed at 24 h and 48 h and (b) MTS proliferation assay was performed at days 2 and 4 post starvation. Values are mean ± SEM obtained from $n = 3$ rats. (C) Western blot analysis of VEGFR2 and VEGFR3 expression in whole lung lysates. Lower panel shows the densitometry analysis graphs. Values are mean ± SEM from $n \geq 3$ rats. (D) Immunofluorescence staining of paraffin-embedded lung sections for VEGFR3 (red fluorescence) and vWF (green fluorescence).

Notes: Arrows show colocalization of vWF and VEGFR3. Scale bar = 50 μm.

****: $p < 0.0001$; ***: $p < 0.001$; **: $p < 0.01$; *: $p < 0.05$ vs control; ###: $p < 0.001$ vs Sugen; $$: $p < 0.01$ vs morphine; SuMo: Sugen–morphine; VEGFR: vascular endothelial growth factor receptor..

both at days 2 and 4 in 0.5% serum containing media (Fig. 3(b)). These results suggest that the combined SuMo administration explains the proliferative capacity of ECs in vitro, and that the combination treatment is responsible for the lumen obliteration by ECs observed in the SuMo rats.

Lungs from SuMo rats show high VEGF receptor expression

VEGFR blockade resulting in initial endothelial apoptosis and later proliferation of apoptosis-resistant ECs has been associated with the development of angio-obliterative PAH in the Sugen/Hypoxia animal model.[8,23] Furthermore, we previously reported that chronic treatment with morphine results in increased proliferation of ECs with an associated increase in the total and phosphorylated VEGFR2.[20] Therefore, we here analyzed the levels of VEGFR expression in the whole lung rat tissue lysates from all four groups. Although we found only mild increase in VEGFR2 protein, significant increase in the protein expression of VEGFR3 was observed in rat lung tissues from the SuMo group compared to controls as well as when compared with Sugen alone or morphine alone treated groups (Fig. 3(c)). The morphine group also demonstrated a significantly higher VEGFR3 expression when compared to control group (Fig. 3(c)). The expression of VEGFR3 was further confirmed by positive VEGFR3 staining (red fluorescence) colocalizing with vWF-stained ECs (green fluorescence) in the pulmonary vessels of lung tissue sections from SuMo rats (Fig. 3(d)).

Discussion

Our study describes and partially characterizes a novel preclinical PAH model in wild-type male SD rats. In this SuMo model, SU5416 combined with morphine caused PAH that presented with similar hallmarks as seen in human PAH. The RVSP was significantly elevated in the group exposed to the double-hit of morphine and SU5416. The histology showed precapillary pulmonary arteriopathy with adventitial and medial thickening with the lumen occlusion of intra-acinar vessels consisting of smooth muscle and ECs. In addition, isolated lung ECs demonstrated significant apoptosis-resistance in vitro after exposure to SU5416 and morphine in vivo. There was also a VEGFR-2 and -3 increased expression in the lungs from the SU5416–morphine rats. To our knowledge, we have developed a novel ''two-hit'' preclinical PAH model in non-genetically modified rats that does not require hypoxia.

PAH, due to chronic and progressive occlusion of precapillary pulmonary vessels, results in elevated pulmonary vascular resistance and leads to RVH and dysfunction.[8,24]

Clinically, patients with PAH demonstrate elevations of the RVSP and mean pulmonary arterial pressure, and histologically angio-obliterative pre- and intra-acinar pulmonary vascular remodeling.[25] The pathobiology underlying the development of severe human PAH is incompletely understood, predominantly due to the complexity of multiple cell–cell interactions. Relevant animal models should reproduce both the lung vascular histology and the PH observed in humans with severe PAH.

Existing preclinical PAH animal models like the monocrotaline model[26,27] or the SU5416 plus chronic hypoxia (SuHx) model[8,13] that develop plexogenic arteriopathy and angio-obliterative lesions have been useful and advanced our mechanistic understanding of the pathobiology underlying PAH. There are now several models where SU5416 serves as one of two hits as in the Su/OVA, AdTGF-β1/SU5416, and Su/pneumonectomy models. These models support the double-hit hypothesis of PAH development.[13,15,16,28–30] One hypothesis of PAH development, based on animal models, is switching of initial apoptosis-surviving EC to a hyperproliferative apoptosis-resistant phenotype that progresses to complex, angio-obliterative lesions formation.[8,11,13,25]. The study by Taraseviciene-Stewart et al. in 2001 demonstrated a significant increase in the caspase-3 and Terminal deoxynucleotidyl dUTP Nick End Labeling-positive pulmonary ECs in SuHx rats.[13] However, concomitant to the development of severe PH in this model, more PCNA-positive ECs were observed in precapillary occluded vessels. Importantly, they reported the prevention of pulmonary vascular endothelial proliferation and the development of angio-obliterative PH in SuHx rats by a pan-caspase inhibitor.[13]

The VEGFs and its receptors (VEGFRs) likely play a crucial role in the pathogenesis of PAH.[31,32] Complex pulmonary vascular lesions from human PAH patients have shown high expression of VEGF and VEGF receptors.[33,34] There are several splice variants of VEGF/VEGFR that promote different functions.[35] VEGFR-1 predominantly acts as an anti-angiogenic factor, while VEGFR2 and VEGFR3 are important in promoting angiogenesis.[36,37] The VEGF ligands A, B, C, and D bind to these receptors to mediate their mitogenic, pro-survival, and angiogenic abilities. VEGF-B binds to VEGFR1, and VEGF-A predominantly binds to VEGFR2 upon activation by phosphorylation through receptor tyrosine kinases and regulate EC proliferation through activation of proliferative signaling pathways like PI3/AKT, ErK1/2 MAP Kinases, and inhibiting caspase-3/Bcl2-mediated EC death and apoptosis.[33] VEGF-C ligand binds to VEGFR3 and has been elucidated to promote endothelial tip cell sprouting, a critical event in the process of angiogenesis.[23,31,38] Over the years, it has been demonstrated that blockade of VEGFR1 and VEGFR2 by SU5416 causes initial endothelial apoptosis, and a second trigger like hypoxia drives the proliferation of apoptosis-resistant cells leading to development of severe PAH. The findings reported by Al-Husseini et al. showed that there is a high VEGFR3 expression in SuHx rat model of PAH, as SU5416 only inhibits VEGFR1 and VEGFR2.[23] VEGFR3, which can get activated without active phosphorylation, remains uninhibited and alternatively can interact with VEGF-C ligand to cause angio-obliterative lesions as observed in the Sugen/hypoxia model of PAH.[23] Similarly, we also observed high expression of VEGFR3 in lung tissues from SuMo rats, supporting a possible mechanism of VEGFR3-mediated endothelial proliferation.

Furthermore, the dual proapoptotic and survival-enhancing action of morphine of ECs has also been earlier described.[17] We earlier demonstrated that morphine, independently as well as in combination with HIV-proteins, can cause initial apoptosis and later proliferation of ECs both in the cell culture system as well as in SIV-infected macaques. Similarly, isolated ECs from rats with a dual hit of Sugen and morphine also showed higher survival and proliferative ability in response to the stress from serum starvation as compared to control rats.

In summary, this study introduces a novel preclinical PAH model in SD rats exposed to a double-hit of morphine and SU5416 that demonstrates multiple characteristics of the human disease. These include significant smooth muscle hypertrophy of proximal vessels, new intimal lesions in intra-acinar arteries, and RV hypertrophy with a moderate increase in the RVSP. We speculate that a more chronic administration with the same or higher non-toxic doses of morphine may worsen the hemodynamic changes in these rats. This novel model will provide an opportunity to further investigate the PAH pathogenesis and it also suggests that opioids might play a role in pulmonary vascular diseases.

Conflict of interest

The author(s) declare that there is no conflict of interest.

Funding

This research received no specific grant from any funding agency in the public, commercial, or not-for-profit sectors.

ORCID iD

Tyler Nguyen https://orcid.org/0000-0002-9872-7149

References

1. Orcholski ME, Yuan K, Rajasingh C, et al. Drug-induced pulmonary arterial hypertension: a primer for clinicians and scientists. *Am J Physiol Lung Cell Mol Physiol* 2018; 314: L967–L983.
2. Harter ZJ, Agarwal S, Dalvi P, et al. Drug abuse and HIV-related pulmonary hypertension: double hit injury. *AIDS* 2018; 32: 2651–2667.

3. Simonneau G, Gatzoulis MA, Adatia I, et al. Updated clinical classification of pulmonary hypertension. *J Am Coll Cardiol* 2013; 62: D34–D41.
4. Borgdorff MA, Dickinson MG, Berger RM, et al. Right ventricular failure due to chronic pressure load: what have we learned in animal models since the NIH working group statement? *Heart Fail Rev* 2015; 20: 475–491.
5. Lahm T, Douglas IS, Archer SL, et al. Assessment of right ventricular function in the research setting: knowledge gaps and pathways forward. An Official American Thoracic Society Research Statement. *Am J Respir Crit Care Med* 2018; 198: e15–e43.
6. Stenmark KR, Meyrick B, Galie N, et al. Animal models of pulmonary arterial hypertension: the hope for etiological discovery and pharmacological cure. *Am J Physiol Lung Cell Mol Physiol* 2009; 297: L1013–L1032.
7. Abe K, Toba M, Alzoubi A, et al. Formation of plexiform lesions in experimental severe pulmonary arterial hypertension. *Circulation* 2010; 121: 2747–2754.
8. de Raaf MA, Schalij I, Gomez-Arroyo J, et al. SuHx rat model: partly reversible pulmonary hypertension and progressive intima obstruction. *Eur Respir J* 2014; 44: 160–168.
9. Itokawa T, Nokihara H, Nishioka Y, et al. Antiangiogenic effect by SU5416 is partly attributable to inhibition of Flt-1 receptor signaling. *Mol Cancer Ther* 2002; 1: 295–302.
10. Fong TA, Shawver LK, Sun L, et al. SU5416 is a potent and selective inhibitor of the vascular endothelial growth factor receptor (Flk-1/KDR) that inhibits tyrosine kinase catalysis, tumor vascularization, and growth of multiple tumor types. *Cancer Res* 1999; 59: 99–106.
11. Sakao S, Taraseviciene-Stewart L, Lee JD, et al. Initial apoptosis is followed by increased proliferation of apoptosis-resistant endothelial cells. *FASEB J* 2005; 19: 1178–1180.
12. Spiekerkoetter E, Tian X, Cai J, et al. FK506 activates BMPR2, rescues endothelial dysfunction, and reverses pulmonary hypertension. *J Clin Invest* 2013; 123: 3600–3613.
13. Taraseviciene-Stewart L, Kasahara Y, Alger L, et al. Inhibition of the VEGF receptor 2 combined with chronic hypoxia causes cell death-dependent pulmonary endothelial cell proliferation and severe pulmonary hypertension. *FASEB J* 2001; 15: 427–438.
14. Happe CM, de Raaf MA, Rol N, et al. Pneumonectomy combined with SU5416 induces severe pulmonary hypertension in rats. *Am J Physiol Lung Cell Mol Physiol* 2016; 310: L1088–L1097.
15. Nicolls MR, Mizuno S, Taraseviciene-Stewart L, et al. New models of pulmonary hypertension based on VEGF receptor blockade-induced endothelial cell apoptosis. *Pulm Circ* 2012; 2: 434–442.
16. Mizuno S, Farkas L, Al Husseini A, et al. Severe pulmonary arterial hypertension induced by SU5416 and ovalbumin immunization. *Am J Respir Cell Mol Biol* 2012; 47: 679–687.
17. Hsiao PN, Chang MC, Cheng WF, et al. Morphine induces apoptosis of human endothelial cells through nitric oxide and reactive oxygen species pathways. *Toxicology* 2009; 256: 83–91.
18. Ding WG, Zhou HC, Cui XG, et al. Anti-apoptotic effect of morphine-induced delayed preconditioning on pulmonary artery endothelial cells with anoxia/reoxygenation injury. *Chin Med J (Engl)* 2008; 121: 1313–1318.
19. Gupta K, Kshirsagar S, Chang L, et al. Morphine stimulates angiogenesis by activating proangiogenic and survival-promoting signaling and promotes breast tumor growth. *Cancer Res* 2002; 62: 4491–4498.
20. Spikes L, Dalvi P, Tawfik O, et al. Enhanced pulmonary arteriopathy in simian immunodeficiency virus-infected macaques exposed to morphine. *Am J Respir Crit Care Med* 2012; 185: 1235–1243.
21. Dalvi P, Sharma H, Chinnappan M, et al. Enhanced autophagy in pulmonary endothelial cells on exposure to HIV-Tat and morphine: role in HIV-related pulmonary arterial hypertension. *Autophagy* 2016; 12: 2420–2438.
22. Fulton RM, Hutchinson EC and Jones AM. Ventricular weight in cardiac hypertrophy. *Br Heart J* 1952; 14: 413–420.
23. Al-Husseini A, Kraskauskas D, Mezzaroma E, et al. Vascular endothelial growth factor receptor 3 signaling contributes to angioobliterative pulmonary hypertension. *Pulm Circ* 2015; 5: 101–116.
24. Pietra GG, Capron F, Stewart S, et al. Pathologic assessment of vasculopathies in pulmonary hypertension. *J Am Coll Cardiol* 2004; 43: 25S–32S.
25. Masri FA, Xu W, Comhair SA, et al. Hyperproliferative apoptosis-resistant endothelial cells in idiopathic pulmonary arterial hypertension. *Am J Physiol Lung Cell Mol Physiol* 2007; 293: L548–L554.
26. Schultze AE and Roth RA. Chronic pulmonary hypertension – the monocrotaline model and involvement of the hemostatic system. *J Toxicol Environ Health B Crit Rev* 1998; 1: 271–346.
27. Gomez-Arroyo JG, Farkas L, Alhussaini AA, et al. The monocrotaline model of pulmonary hypertension in perspective. *Am J Physiol Lung Cell Mol Physiol* 2012; 302: L363–L369.
28. Daley E, Emson C, Guignabert C, et al. Pulmonary arterial remodeling induced by a Th2 immune response. *J Exp Med* 2008; 205: 361–372.
29. Farkas L, Farkas D, Ask K, et al. VEGF ameliorates pulmonary hypertension through inhibition of endothelial apoptosis in experimental lung fibrosis in rats. *J Clin Invest* 2009; 119: 1298–1311.
30. Taraseviciene-Stewart L, Nicolls MR, Kraskauskas D, et al. Absence of T cells confers increased pulmonary arterial hypertension and vascular remodeling. *Am J Respir Crit Care Med* 2007; 175: 1280–1289.
31. Voelkel NF and Gomez-Arroyo J. The role of vascular endothelial growth factor in pulmonary arterial hypertension. The angiogenesis paradox. *Am J Respir Cell Mol Biol* 2014; 51: 474–484.
32. Voelkel NF, Vandivier RW and Tuder RM. Vascular endothelial growth factor in the lung. *Am J Physiol Lung Cell Mol Physiol* 2006; 290: L209–L221.
33. Tuder RM, Chacon M, Alger L, et al. Expression of angiogenesis-related molecules in plexiform lesions in severe pulmonary hypertension: evidence for a process of disordered angiogenesis. *J Pathol* 2001; 195: 367–374.
34. Hirose S, Hosoda Y, Furuya S, et al. Expression of vascular endothelial growth factor and its receptors correlates closely

with formation of the plexiform lesion in human pulmonary hypertension. *Pathol Int* 2000; 50: 472–479.
35. Ferrara N, Gerber HP and LeCouter J. The biology of VEGF and its receptors. *Nat Med* 2003; 9: 669–676.
36. de Vries C, Escobedo JA, Ueno H, et al. The fms-like tyrosine kinase, a receptor for vascular endothelial growth factor. *Science* 1992; 255: 989–991.
37. Kendall RL and Thomas KA. Inhibition of vascular endothelial cell growth factor activity by an endogenously encoded soluble receptor. *Proc Natl Acad Sci USA* 1993; 90: 10705–10709.
38. Tammela T, Zarkada G, Wallgard E, et al. Blocking VEGFR-3 suppresses angiogenic sprouting and vascular network formation. *Nature* 2008; 454: 656–660.